(Abstract submitted to the 34th IWWWFB, Australia, 2019)

Modelling of Wave-structure Interaction for Cylindrical Structures using a Spectral Element Multigrid Method

Wojciech Laskowski[1], Harry B. Bingham[3] and Allan P. Engsig-Karup[1,2]
[1] Department of Applied Mathematics and Computer Science
[2] Center for Energy Resources Engineering (CERE)
[3] Department of Mechanical Engineering
Technical University of Denmark, 2800 Kgs. Lyngby, Denmark.
(wola,hbb,apek)@dtu.dk

Highlights

- Time-domain modeling of wave-structure interaction for surface-piercing bottom-mounted and truncated cylindrical structures.
- Fully Nonlinear Potential Flow (FNPF) time domain solver based on a high-order Spectral Element Method that has support for geometric flexibility using adaptive meshes and high-order convergence rates.
- Efficient and scalable $\mathcal{O}(n)$ solution effort using a geometric p-multigrid method that enables practical calculation times for engineering analysis.

Introduction

The need for advanced time-domain simulators for improved offshore engineering analysis is growing with the continued improvement in computational resources. In line with this trend, we consider a fully nonlinear potential flow (FNPF) model discretised with a stabilised Galerkin Spectral Element Method (SEM) [5] addressing the stability problems and lack of progress made for this type of modelling approach since the work of Robertson & Sherwin (1999) [9]. A recent review of the SEM is given in [12] and the benefits of high-order discretizations and multigrid for FNPF models are well-known, e.g. see [1, 2]. In a recent study, a SEM-based FNPF model (FNPF-SEM) model [4] was developed and then validated in a blind test experiment against experimental measurements for focusing waves interacting with a fixed FPSO structure. In this work, we consider a standard benchmark problem for cylindrical structures due to McCamy & Fuchs (1954), with the objective of evaluating an entirely new extension of this solver with a p-multigrid method which enables scalable $\mathcal{O}(n)$ complexity in work effort. Recently, the first proof of an efficient geometric p-multigrid method was demonstrated in 2D/3D [7], and in this work we provide some additional results with the aim of demonstrating the *practical feasibility* of using this new SEM-based solver for 3D analysis. In particular, the new FNPF-SEM p-multigrid solver makes it possible to address both wave propagation and wave-structure problems within a single solver. The p-multigrid method is designed to exploit the p-type convergence property in solving the Laplace problem, and by avoiding an h-type convergence strategy, it is possible to handle the representation of structural bodies with curvilinear features without refining the underlying mesh-topology. In this sense, this work contributes to demonstrating that the SEM can be an efficient basis for a technology that is useful for engineering analysis. It comes with the ability to represent offshore structures and the discretization leads to sparse matrices after global assembly in the discrete problem, and therefore can be solved iteratively with high parallel efficiency and scalability. By using a FNPF formulation it is possible to predict the wave-induced horizontal and vertical hydrodynamic forces on offshore structures, and account for the nonlinear effects that are significant when standard frequency domain analysis falls short.

Governing equations

We consider the Eulerian formulation based on fully nonlinear potential flow theory [3]. A Cartesian coordinate system is adopted with the origin on the still water xy-plane and the z-axis pointing vertically upwards. t is time. The fluid domain is bounded by the sea bottom at $z = -h(\mathbf{x})$, the free-surface at $z = \eta(\mathbf{x}, t)$, and an enclosing boundary that defines the dimensions of a Numerical Wave Tank (NWT) as well as the structural boundaries. The free surface boundary conditions are expressed in terms of 'free-surface only' variables

$$\frac{\partial}{\partial t}\eta = -\nabla\eta\cdot\nabla\tilde{\phi} + \tilde{w}(1+\nabla\eta\cdot\nabla\eta), \quad (1a)$$

$$\frac{\partial}{\partial t}\tilde{\phi} = -g\,\eta - \frac{1}{2}\nabla\tilde{\phi}\cdot\nabla\tilde{\phi} + \frac{1}{2}\tilde{w}^2(1+\nabla\eta\cdot\nabla\eta). \quad (1b)$$

Here $\nabla = (\partial/\partial x, \partial/\partial y)$ is the horizontal gradient operator, g the gravitational acceleration. These equations describes the temporal evolution of the free surface elevation η and velocity potential $\tilde{\phi}$. Subject to numerical discretization, these equations can be solved efficiently using a classical explicit fourth-order Runge-Kutta method. To obtain closure, the vertical velocity at the free surface $\tilde{w}$ is determined from the known state of the fluid surface defined by η and $\tilde{\phi}$, that requires satisfying a continuity equation (Laplace equation) and solid boundary conditions.

$$\nabla^2\phi + \phi_{zz} = 0, \qquad -h(x,y) \le z \le \eta(x,y,t) \quad (2a)$$

$$\phi_z + \nabla h\cdot\nabla\phi = 0, \qquad z = -h(x,y). \quad (2b)$$

$$\mathbf{n}\cdot(\nabla\phi, \phi_z) = 0, \qquad \text{on } \Gamma_b, \quad (2c)$$

where $\boldsymbol{n}$ represents the outward pointing normal vector at structural surfaces Γ_b.

This Laplace problem is discretized using a Spectral Element discretization where the fluid volume (domain) is decomposed into a set of non-overlapping elements. These elements are taken to be prism elements in two layers that are generated using the mesh generator `Gmsh`. The elements in the bottom layer are kept fixed and in the upper layer adjusted to the free surface using elements stretched with the position of the curvilinear free surface at a given instant of time. Across the domain, solution quantities are represented using global finite element basis functions that are globally piece-wise continuous polynomial basis functions of arbitrary polynomial order. This discretization [4] leads to a system of equations that defines the discrete Laplace problem

$$\boldsymbol{L}\boldsymbol{\phi} = \boldsymbol{b}, \quad \boldsymbol{L} \in \mathbb{R}^{n\times n}, \quad \boldsymbol{b} \in \mathbb{R}^n. \quad (3)$$

This problem is a computational bottleneck in our procedure and we solve it efficiently using a geometric p-multigrid method tailored to the MarineSEM library, and is exploited specifically as an iterative solver in the FNPF-SEM model.

Geometric p-multigrid method

A recursive version of multi-level p-multigrid method is implemented based on a standard V-cycle algorithm, described in [11]. Consider the span of P grids $\{\Omega_1, ..., \Omega_P\}$ that discretize the same spatial domain by the same set of non-overlapping shape regular elements, but with different orders of the polynomial basis functions in each spatial direction $\boldsymbol{N}_p = (N_{p,1}, N_{p,2}, N_{p,3})$, such that $\forall\ 1 \le p \le P,\ 1 \le i \le 3\ :\ N_{p,i} > N_{p-1,i}$. Instead of solving the full linear system 3, we exploit the SE discretization properties and exclude the interior nodes of the elements. This method is known as *Static Condensation* [6] and leads to a better conditioned system of equations with fewer degrees of freedom. The implemented solver requires two main

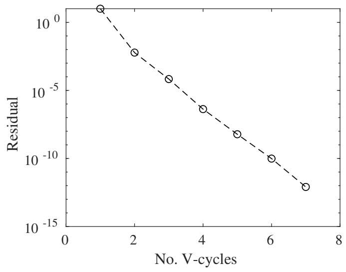

Figure 1: Averaged residual plot during 100 time steps.

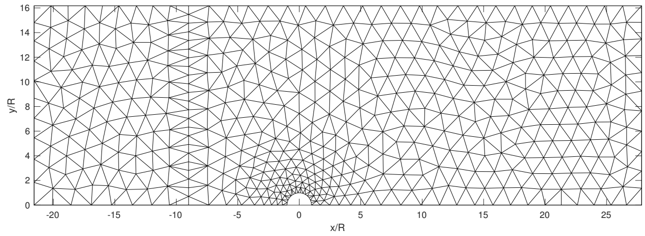

Figure 2: Illustration of mesh. Free surface plane including a wave generation zone.

(a) Wave envelope

(b) Wave runup

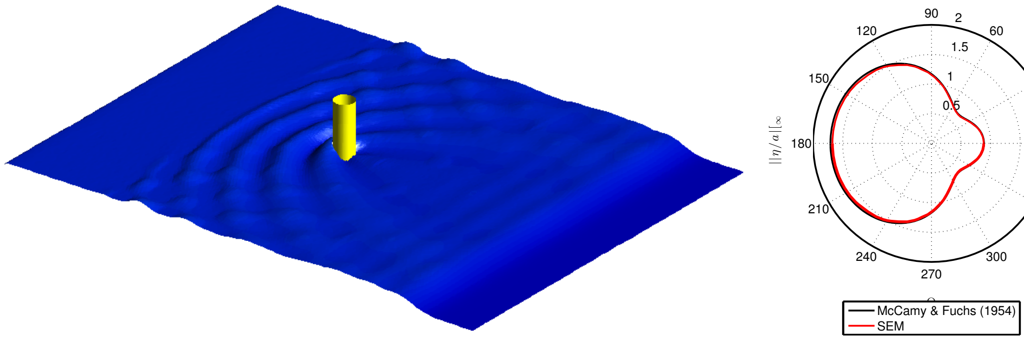

Figure 3: (a) Wave envelope with some visible reflections near boundaries away from the proximity of the cylinder. (b) Comparison of maximum wave run-up on a mono-pile in an open sea for MF solution and computed results shows excellent agreement. $kh = 1$. $kR = 1$. Maximum wave run-up is predicted to be up to 1.67 times larger on front side relative to the incident wave amplitude as determined from the wave crest envelope. Polynomial expansion orders $(N_{xy}, N_z) = (5, 6)$ on elements. $\Delta t = 0.02$ s.

components: grid transfer operators and smoothers. In the p version of multi-level solver, prolongation $\boldsymbol{P}_{p-1}^{p} : \Omega_{p-1} \rightarrow \Omega_p$ is a local operation (defined in elemental space) representing the higher-order basis function in therms of the lower-order basis [10] and suited for the Continuous Galerkin Spectral Element framework. The restriction operator is its transpose $\boldsymbol{R}_p^{p-1} = (\boldsymbol{P}_{p-1}^{p})^T : \Omega_p \rightarrow \Omega_{p-1}$, cf. [10]. The choice of polynomial orders on each level p and the total number of grids P, also known as the *coarsening strategy*, is optimised in terms of computational cost and tailored for a particular mesh and input parameters. Consider smoothing on each level p as ν preconditioned Richardson iterations: $\hat{\boldsymbol{\phi}}_p^{m+1} \leftarrow \hat{\boldsymbol{\phi}}_p^{m} + \boldsymbol{M}(\hat{\boldsymbol{b}}_p - \hat{\boldsymbol{L}}_{\boldsymbol{p}} \hat{\boldsymbol{\phi}}_p^{m}),\ m = 0, ..., \nu - 1$. In this study, we examine the performance of the standard relaxation schemes (Jacobi, Gauss-Seidel) and also modern block techniques in the form of Weighted Additive Schwarz methods [6, 8]. In order to enhance the performance and robustness on anisotropic meshes, we deploy p-multigrid as a preconditioner to the outer iterative solver, e.g. the defect correction or Krylov subspace methods [8, 2].

Numerical experiments

The main purpose of the numerical experiments is to validate the numerical model and highlight the high accuracy and flexibility of the model for nonlinear wave propagation and wave-structure interactions. We consider the scattering of regular waves on a single cylinder in an open sea with flat bottom. We compare to the exact solutions due to McCamy & Fuchs (1954) (MF) valid for a cylinder positioned in finite depth. This MF solution for small amplitude waves generalises the solution of Havelock (1940) for a cylinder in deep water. The validity of this study on diffraction effects lies in the assumption that the inertial forces dominate the drag forces in interaction of the fluid with the cylinder. The case highlights the ability of the SEM to accurately account for the circular boundary representation of a realistic shape of an object such as a mono-pile foundation, cf. Fig. 2. We consider a case for predicting the maximum wave run-up assuming small amplitude wave propagation at relative depth $kh = 1$ and relative size of cylinder $kR = \pi/2$. Excellent agreement between the analytical results of MF and the SEM solution is given in Fig. 3. In the simulation we have used curvilinear iso-parametric elements to represent the cylinder boundary. The minor discrepancy in the wave run-up at the front side is due to minor reflections between the wave generation zone and the cylinder. The result demonstrates the accuracy that can be achieved using the SEM model. The p-multigrid solver efficiency is highlighted in Fig. 1. At the workshop we plan to demonstrate results for cases describing the interaction between nonlinear waves and cylindrical structures.

References

[1] H. B. Bingham and H. Zhang. On the accuracy of finite-difference solutions for nonlinear water waves. *J. Engineering Math.*, 58:211–228, 2007.

[2] A. P. Engsig-Karup. Analysis of efficient preconditioned defect correction methods for nonlinear water waves. *International Journal for Numerical Methods in Fluids*, 74(10):749–773, 2014.

[3] A. P. Engsig-Karup, L. S. Glimberg, A. S. Nielsen, and O. Lindberg. Fast hydrodynamics on heterogenous many-core hardware. In Raphäel Couturier, editor, *Designing Scientific Applications on GPUs*, Lecture notes in computational science and engineering. CRC Press / Taylor & Francis Group, 2013.

[4] A.P. Engsig-Karup and C. Eskilsson. Spectral element fnpf simulation of focused wave groups impacting a fixed fpso. In *Proceedings of The Annual International Offshore and Polar Engineering Conference (ISOPE) 2018*, Japan, 2018.

[5] Eskilsson C. Engsig-Karup, A. P. and D. Bigoni. A stabilised nodal spectral element method for fully nonlinear water waves. *J. Comp. Phys.*, 318:1–21, 2016.

[6] L. Haupt, J. Stiller, and W.E. Nagel. A fast spectral element solver combining static condensation and multigrid techniques. *Journal of Computational Physics*, 255:384 – 395, 2013.

[7] W. Laskowski. Designing efficient p-multigrid strategies forthe laplace equation - with application to aspectral element fully nonlinear potentialflow model. Master's thesis, Department of Applied Mathematics and Computer Science, Technical University of Denmark, 2018.

[8] James W. Lottes and Paul F. Fischer. Hybrid multigrid/schwarz algorithms for the spectral element method. *Journal of Scientific Computing*, 24(1):45–78, Jul 2005.

[9] I. Robertson and S. Sherwin. Free-surface flow simulation using hp/spectral elements. *J. Comput. Phys.*, 155:26–53, 1999.

[10] Einar M. Rønquist and Anthony T. Patera. Spectral element multigrid. i. formulation and numerical results. *Journal of Scientific Computing*, 2(4):389–406, Dec 1987.

[11] U. Trottenberg, C. W. Oosterlee, A. Schuller, contributions by A. Brandt, P. Oswald, and K. Stuben. *Multigrid*. Academic Press, San Diego, CA, 2001.

[12] H. Xui, C.D. Cantwell, C. Monteserin, C. Eskilsson, A.P. Engsig-Karup, , and S. J. Sherwin. Spectral/hp element methods: Recent developments, applications, and perspectives. *Journal of Hydrodynamics*, 30(1):1–22, 2018.